Preprints of the 2012 20th Mediterranean Conference on Control & Automation (MED), Barcelona, Spain, July 3-6, 2012

Influence of the Inverter Control-System to the Mechanical and Electrical Behaviour of an Electric Vehicle modulated as a Two-Mass-System

Philip Dost[1] and Constantinos Sourkounis[2]

Abstract— **The current developments for the energy supply of individual mobility are emerging electrical energy as an energy source for electric drives [1]. Due to these developments there is a need of considering the conditioning of electrical energy to be used for electrical machines under conditions of an electric vehicle. Comparing a fixed step-size control-system with a hysteresis-control (bang-bang-control), the high frequent influence to the whole power train is evaluated with a view to the electrical and mechanical drive train [2]. Furthermore the travelling comfort is a target of the study [3].**

As electrical drives for electric vehicles need to have a wide speed range and likewise be robust the chosen control processes are applied to a permanent magnet excited synchronous machine (PMSM) [4], [5]. This offers the opportunity of a gear-less drive. This by the way offers a big advantage in comparison to combustion engines. To connect the energy source to the PMSM an inverter is used. This builds three-phases for the machine and likewise a rectifier in the opposed direction to the battery. The Inverter is built with a set of IGBTs (Insulated Gate Bipolar Transistor) and integrated anti parallel diodes. The command signal is set by a torque demand, as known in a traditional car, with the help of an acceleration pedal [6], [7]. The mechanical part of the drive train is realized as a double oscillator as this represents the real mechanical drive train.

I. Introduction

According to the political influence a new generation of passenger cars joins the market with increasing influence. These cars are based on electrical machines and most of them are using a battery as their energy source. Hence these cars are much more quick developed than well organized, there is a need to optimize the used strategies. This paper concentrates on well known pulsing methods which are fitted to the use within an electric vehicle (ev).

These pulsing methods control the inverter within the ev's drive train and are necessary for conditioning the output current for the machine.

To work out the best choice of the control strategy there is a comparison of a fixed step size control as well as a non deterministic control. This happens with respect to the double oscillator in the mechanical part of the drive train. This possess a big influence to the mechanical vibrations in the car.

[1]P. Dost is with Faculty of Electrical Engineering and Information Technology, Power Systems Technology and Power Mechatronics, 44801 Bochum, Germany dost@emesys.rub.de

[2]C. Sourkounis is with Faculty of Electrical Engineering and Information Technology, Power Systems Technology and Power Mechatronics, 44801 Bochum, Germany office@enesys.rub.de

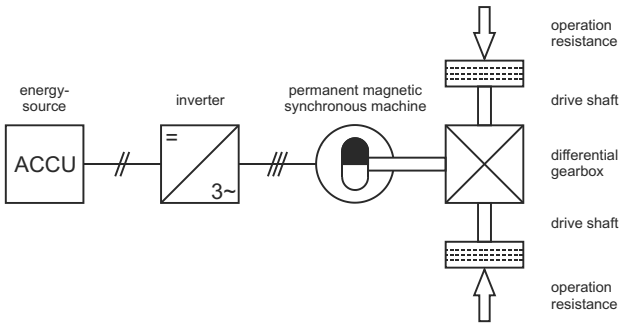

Fig. 1. Power train of an electric operating vehicle

II. Set up of the electrical drives in an electric vehicle

A. Electrical Elements

To avoid different conditions for the comparison of the control processes the energy source is set up to an ideal voltage source with unlimited current output. The direct current voltage output of the source is $600\,\mathrm{V}$. This set up offers the opportunity to integrate a wide range of energy sources that offer a voltage source into the power train. For example the integration of accumulators or fuel cells are able to assimilate as well as solar panels or hybrid systems. The dimensions of the PMSM are set up to reach a maximum speed of $6000\,\mathrm{rpm}$ which offers a maximum locomotion speed of $180\,\mathrm{km/h}$ [8] [9]. This is offered due to an integrated gearbox with a transmission of 3.227 having a set of tyres with the dimensions of $195/55R16$. Further settings are the pairs of poles which are defined to $p = 2$, the stator resistance R_s to $0.05\,\Omega$, the magnetic flux to $\Psi_{PM} = 1/3\,\mathrm{Wb}$ as well as the equivalent inductivities L_d and L_q which are determined to $1.98\,\mathrm{mH}$ [10]. The implemented inertia is determined to $0.033\,\mathrm{kg}\cdot\mathrm{m}^2$. Further on the rotor axis related inertia of the cars mass is $6.33\,\mathrm{kg}\cdot\mathrm{m}^2$. The friction factor of the machine is $0.0003\,\mathrm{Nms}$. To calculate the torque (M) of a PMSM as a function of the current components (i_d and i_q) and the speed (ω_l) the following equations are given (see. eqns. 1, 2 and 3).

$$M = \frac{3}{2} p (I_q \Psi_d - I_d \Psi_q) \tag{1}$$

978-1-4673-2529-5/12/$31.00 ©2012 IEEE

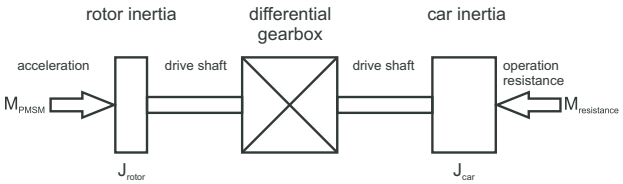

Fig. 2. Mechanical elements of the power train of an electric operating vehicle

$$u_d = I_d R + \frac{\mathrm{d}\Psi_d}{\mathrm{d}t} - \omega_l \Psi_q$$
$$u_q = I_q R + \frac{\mathrm{d}\Psi_q}{\mathrm{d}t} + \omega_l \Psi_d \quad (2)$$

$$\Psi_d = I_d L_d + \Psi_{PM}$$
$$\Psi_q = I_q L_q \quad (3)$$

The operating resistance of the power train is implemented by air drag in terms of an external speed dependent torque (see. fig. 1) [11]. The inverter components are set to an on-resistance R_{on} of $1\,\mathrm{m\Omega}$ and a snubber-resistance R_s of $100\,\mathrm{k\Omega}$ for each of the IGBTs including the anti parallel diodes. The components set up constitutes a three-phase inverter and a rectifier in the opposite direction. The reluctance drops are not considered.

B. Mechanical Elements

With respect to the damping and stiffness of the axis it is integrated in the model as a two mass oscillator (see. fig. 2) including the differential gearbox. By this the axis is realized as a damping element with $2500\,\mathrm{Nm}\cdot\mathrm{s/rad}$ and a stiff element with $2000\,\mathrm{Nm/rad}$. Due to the recognition of the two mass oscillator the mechanical behaviour of the car body is easier to realize. [12]

The implemented stiffness (see. fig. 3) leads to a resonance frequency of

$$w_{ef} = \frac{1}{T_{ef}} = \sqrt{C\left(\frac{1}{J_{rotor}} + \frac{1}{J_{car}}\right)} = 246.25\,\mathrm{Hz} \quad (4)$$

which means a time constant of

$$T_{ef} = 4.061\,\mathrm{ms}. \quad (5)$$

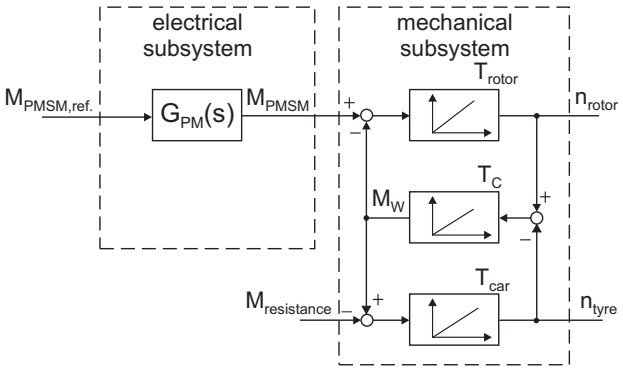

Fig. 3. Block diagram of the pant of the two mass oscillator

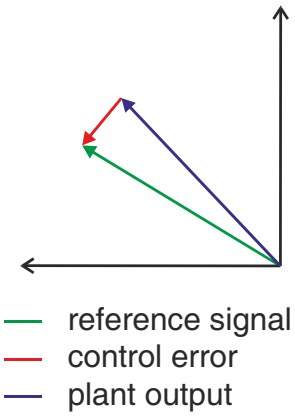

Fig. 4. illustratoin of the reference vector and the plant output and the resulting control error

As this frequency is the resonance frequency, is should be avoided to be induced to the mechanical drive train.

III. Assimilate the Inverter Control Structure

To create a three-phase alternating current the inverter has to obtain switching signals by an external control device. To compare a fixed step size control process with a control process of variable step size the chosen processes are a pulse wide modulation [9], [13], [14] and a stator orientated bang-bang-control [15].

A. Implementation of space vector modulation

The space vector modulation is based on the stator based coordinate system. Based on a reference signal and the plant output an control error is calculated

All vectors are space vectors. The control error space vector builds the basis for the plant input for the next control sequence. This means based on a pwm- (pulse width modulation) signal the control error has to be minimized within a single time slot by switching space vectors. In an ideal case the control error would be dissolved. But Due to the rotor rotation a new control error arises constantly. Due to this constant modulation of space vectors the name “space vector modulation” was built.

To lead the plant output to the reference input value within a single time slot the best way would be to set a space vector in direction of the control error. But due to the inverter there are only six discrete space vectors and two additional zero voltage space vectors.

To achieve setpoint following nevertheless, two space vectors has to be taken to be switched one after another. The chosen space vectors must be proper to rebuild the control error space vector. The space vectors to be chosen are the nearest space vectors to the control error. Choosing the proper time both for combining those space vectors, it is easily possible to rebuilt the control error space vector.

In addition to the direction of the control error the length of this space vector has to be taken into concern. To reach the proper length zero voltage space vectors are used at the

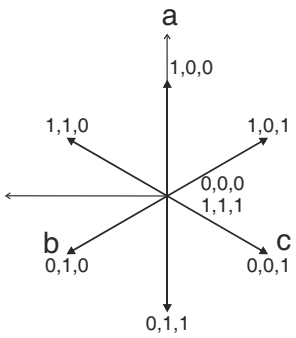

Fig. 5. Space vectors based on the implemented inverter

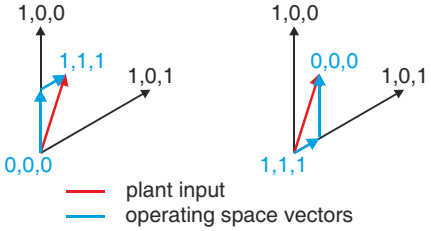

Fig. 6. Modulation of the space vector

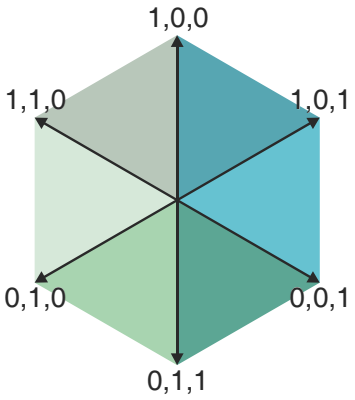

Fig. 7. Sectors to choose the space vectors

beginning and the end of the modulation step. These zero voltage space vectors do not have any effect on the current.

To reduce the number of switching operations the zero voltage space vectors are alternating between $(0,0,0)$ and $(1,1,1)$. According to this there is a need of three switching operations per time slot which means one per IGBT. To optimize the level control these space vectors are set for the same time span at the beginning or at the end of the time slot. Depending on the starting value there are two possible modulation options. An example is shown in figure 6.

The figure shows the space vector order from $(0,0,0)$ to $(1,0,0)$ to $(1,0,1)$ to $(1,1,1)$. Further on it shows the oposite directon if the starting space vector is $(1,1,1)$. These cycles define the switching frequency of the IGBTs to the pwm frequency which is set to $2\,\mathrm{kHz}$. The chosen space vectors vary depending on the sector in which the control error space vector is situated (see. fig. 7). The adjacent space vectors to the sector have to be chosen.

Finally the relation between the switch on time of the

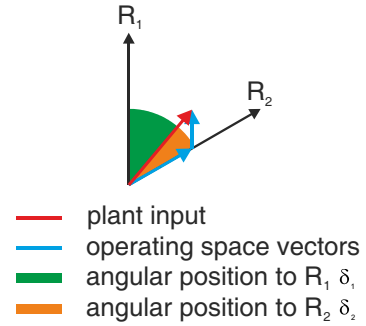

Fig. 8. Angular position within the sector

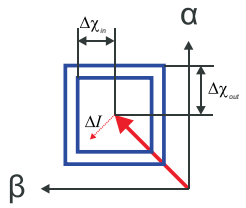

Fig. 9. Tolerance area for the control deviation in the stator orientated bang-bang control

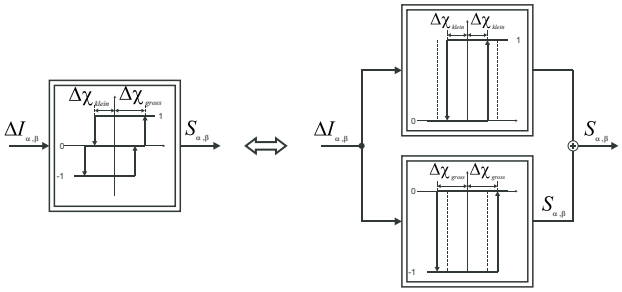

Fig. 10. Hysteretic structure of the stator orientated bang-bang-control

space vectors has to be specified. These depend on the angular position within the sector (see. fig. 8).

According to this the switch on relation can be calculated by

$$\frac{T_{\mathrm{on},R_1}}{T_{\mathrm{on},R_2}} = \frac{\delta_1}{\delta_2}. \tag{6}$$

The time of the zero voltage space vectors has to be regulated with the help of a PI-controller.

[18].

B. Implementation of the bang-bang control

The bang-bang control is realized for stator-orientated values. This means that the tolerance area is spanned in the $\alpha\beta$-coordinate system (see. fig. 9). As the tolerance shape equals a square but there are three IGBTs to control, the tolerance shape has two tolerance steps, for this gives the opportunity to control three different output signals. The built hysteresis structure is a three step hysteresis on which the current components are led (see. fig. 10).

The hysteresis structure finally builds up a signal word with two characters each with three possible values which are minus one, zero and one, so that there are nine different

TABLE I

CONTROL SIGNALS AND SIGNAL OUTPUT OF THE STATOR ORIENTATED BANG-BANG CONTROL

control space vector	S_0	S_1	S_2	S_3	S_4	S_5	S_6	S_7	S_8
S_α	0	1	1	0	-1	-1	-1	0	1
S_β	0	0	1	1	1	0	-1	-1	-1
space vector	U_0	U_4	U_6	U_2	U_2	U_3	U_1	U_5	U_5
alternative	U_7			U_6				U_1	
output signal	0,0,0	1,0,0	1,1,0	0,1,0	0,1,0	0,1,1	0,0,1	1,0,1	1,0,1
alternative	1,1,1			1,1,0				0,0,1	

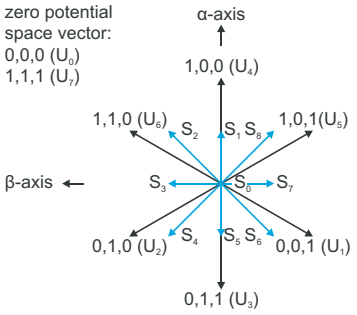

Fig. 11. Signal words of the Hysteresis structure of the stator orientated bang-bang-control

signal words. Besides three signal words any other signal word leads to a specific switching signal which is sent to the inverter. Each of the three exceptions offers different output signals whose choice is based on the signal with the smallest switching effort (see. Tab. I). The switching signals are of that the control deviation is led back into the tolerance area. 11 shows the possible signal words of the control element which lead to the closest space vector which accomplish the dwindling of the control deviation. The space vector is finally kept until the control deviation leaves the tolerance area to another direction. This type of IGBT switching includes a control system without using any additional control structures. The eventuation of the switching operation is stochastic and has thereby no deterministic occasion.

As the tolerance area is stator orientated it has to rotate around the origin of the ordinates (see. fig. 12). The space vector represents the control reference input variable which statically rotates by the same angular velocity as the rotor (see. fig. 10).

IV. BEHAVIOUR AND EVALUATION OF THE INVERTER CONTROL STRUCTURES AT A DOUBLE OSCILLATOR

A. Chosen operating conditions

According to 13 the most meaningful operation points are chosen for a comparison. These are acceleration from standstill, from $50\,\mathrm{km/h}$ and from $100\,\mathrm{km/h}$. The reference torque is set to the nominal torque to analyse and compare the most difficult operating conditions. These records

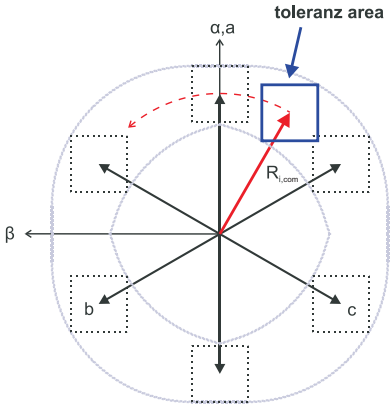

Fig. 12. Hysteresis area of the stator orientated bang-bang-control

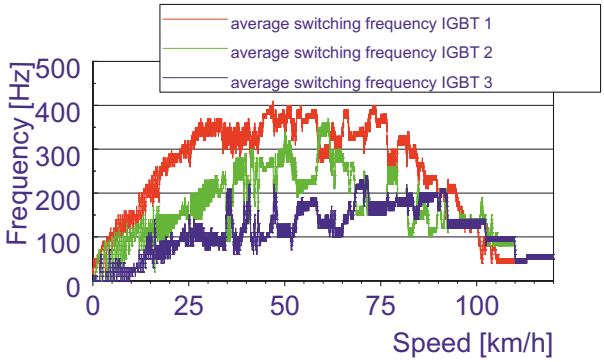

Fig. 13. Average speed dependent switching frequency of the stator orientated bang-bang-control

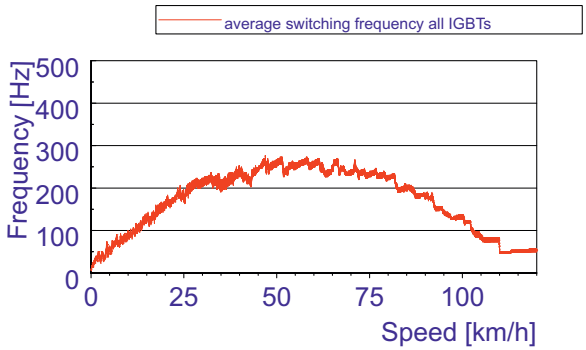

Fig. 14. Average speed dependent switching frequency of the stator orientated bang-bang-control

represent one second acceleration from the respective initial condition.

B. Acceleration with nominal torque from standstill

Fig. 15 shows the differences between the space vector modulation and the bang bang control in the Fourier analysis. This figure shows the comparison of both pulsing methods for the machine torque (see. fig. 17a), the battery current (see. fig. 15b), and the impact to the car represented by the tyres acceleration (see. fig. 15c). At low frequencies the bang bang control shows a higher impact on the torque inducting current and the tyres acceleration than the space vector

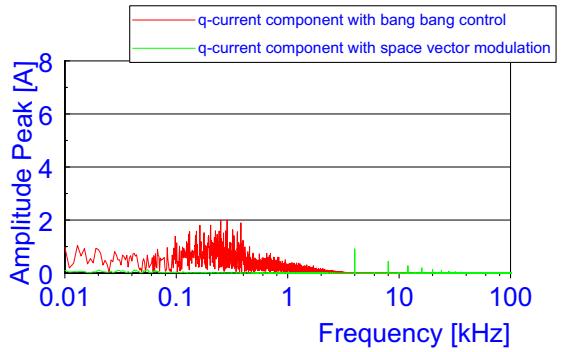

(a) Fourier analyses of the torque inducing current in the machine

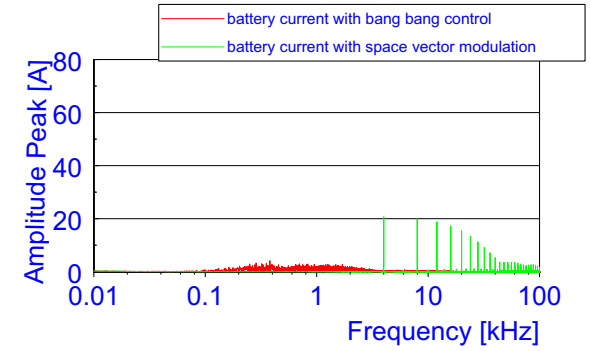

(b) Fourier analyses of the batteries current

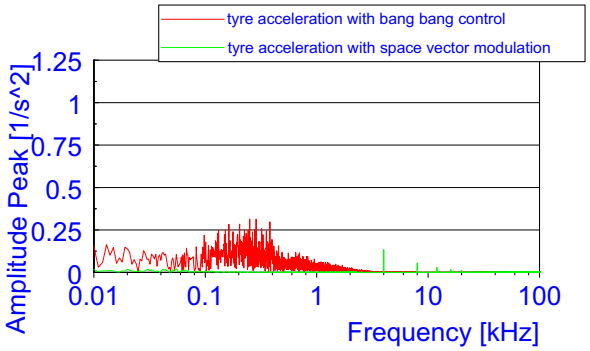

(c) Fourier analyses of the acceleration at the tyre

Fig. 15. Fourier analysis of the signal for 1 s during the acceleration from standstill with nominal torque

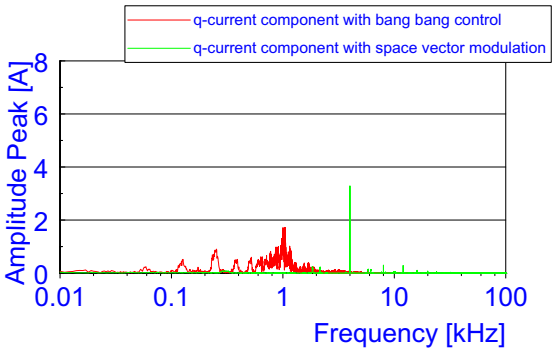

(a) Fourier analyses of the torque inducing current in the machine

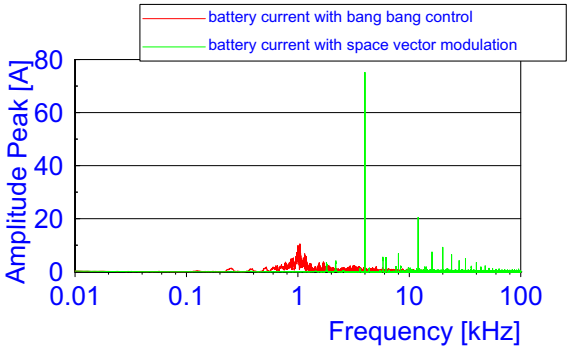

(b) Fourier analyses of the batteries current

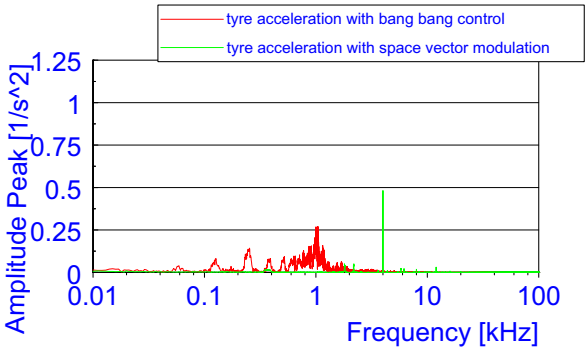

(c) Fourier analyses of the acceleration at the tyre

Fig. 16. Fourier analysis of the signal for 1 s during the acceleration from standstill 50 km/h with nominal torque

modulation. In contrast to that the space vector modulation shows a high impact on the battery. The impact of the space vector modulation to any element starts with frequencies of 4 kHz and above. 4 kHz is the second harmonic to the pwm frequency. This is the highest impact as the side bands of the first harmonic concur at the second harmonic. Higher frequencies caused by the space vector modulation are represented by even harmonics.

C. Acceleration with nominal torque from 50 km/h

Fig. 16 shows the comparison of the measured elements within the car. The measurements are done under the same circumstances as in the previous paragraph (see. eqn. IV-B).

At a speed of 50 km/h the bang bang control has a very low impact on any measured element. In contrast to that the space vector modulation has a high impact at the second harmonic which exceeds the highest amplitude of the bang bang control. Nevertheless the space vector modulation shows only one single harmonic with a high impact. According to this it can be easily realised to filtrate this harmonic.

D. Acceleration with nominal torque from 100 km/h

Finally the acceleration from 100 km/h for one second is contemplated (see. fig. 17). This measurement shows again a very healthy impact on the battery for the bang bang control. In contrast to that the impact on the vehicles torque exceeding any other previous measurement. The space vector modulation has low impact on the battery as well. Further more the impact on the torque is low, too. The second

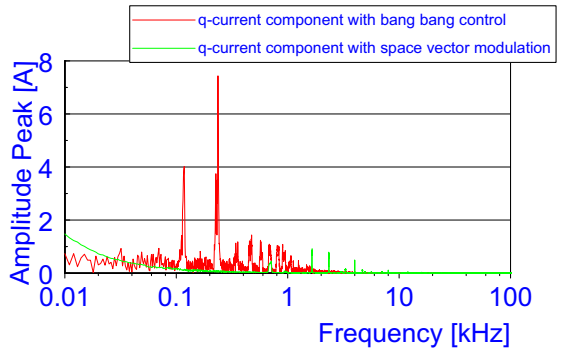

(a) Fourier analyses of the torque inducing current in the machine

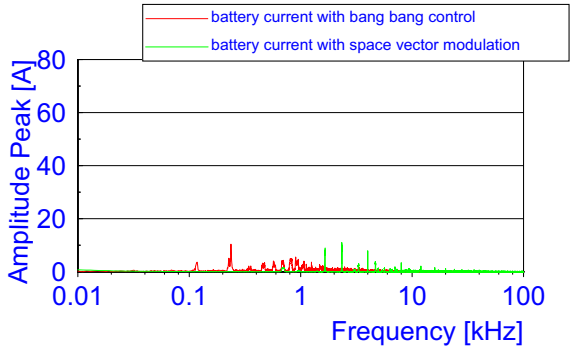

(b) Fourier analyses of the batteries current

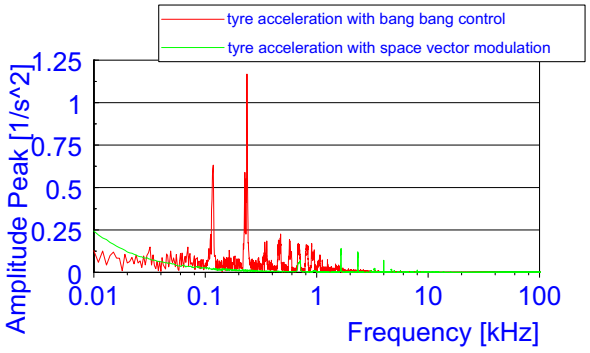

(c) Fourier analyses of the acceleration at the tyre

Fig. 17. Fourier analysis of the signal for 1 s during the acceleration from standstill 100 km/h with nominal torque

harmonic is shrank within this measurement therefore the side-bands of the first harmonic increased slightly.

V. Conclusion

The Measurements have shown that the bang bang control has a high impact on the mechanical part of the drive train. In contrast to that the space vector modulation has a higher impact on the battery system except for the speed of 100 km/h. The current costs for batteries, as well as its high ageing factor of batteries lead to a preferred usage of the bang bang control. On top of that the increase of the switching frequency allows the bang bang control to reduce its mechanical impact. This can be realized by applying a smaller hysteresis range. As a conclusion the bang bang control offers more potential than the space vector modulation. On top of that its lower switching frequencies, in comparison to the 2 kHz of the pwm based space vector modulation, offer a lower power loss in the whole drive train.

References

[1] A. Broy and C. Sourkounis, "Influence of charging electric vehicles and on the quality of the distribution grids," in *Electrical Power Quality and Utilisation (EPQU), 2011 11th International Conference on*, oct. 2011, pp. 1 –4.

[2] C. Sourkounis, "Dynamic torque control in electromechanical drive train with pid-state control," in *Control and Automation, 2009. MED '09. 17th Mediterranean Conference on*, june 2009, pp. 1504 –1510.

[3] C. Soukounis and P. Dost, "Influence to the electrical and mechanical sub system due to inverter control processes on a power train of electric vehicles," in *Power Engineering, Energy and Electrical Drives (POWERENG), 2011 International Conference on*, may 2011, pp. 1 –6.

[4] P. Dost and C. Sourkounis, "Effects of the control-process-structure to the drivability in electric vehicles," in *Control Automation (MED), 2011 19th Mediterranean Conference on*, june 2011, pp. 365 –370.

[5] T. Finken, M. Hombitzer, and K. Hameyer, "Study and Comparison of several Permanent-Magnet excited Rotor Types regarding their Applicability in Electric Vehicles," in *VDE Kongress 2011 - E-Mobility*, Nov. 2010.

[6] Conte, F.V., Giuliani, H., Oberguggenberger, H., and Noll, M., "Modular Design of an Energy Storage System for a Hybrid Electric Vehicle," *Haus der Technik Fachbuch*, vol. 80, pp. 362 –373, 2007.

[7] H. Neudorfer, "Vergleich unterschiedlicher elektrischer Antriebssysteme fr Elektro- und Hybridstraenfahrzeuge," *Neue elektrische Antriebskonzepte fr Hybridfahrzeuge, Haus der Technik Fachbuch*, vol. 80, pp. 234 –263, 2007.

[8] H. C. M. Hennecke, *Htte - Das Ingenieurwissen*. Springer Berlin Heidelberg, Nov. 2007, vol. 0.

[9] D. Schrder, *Elektrische Antriebe - Regelung von Antriebssystemen*. Springer Berlin Heidelberg, 2009, vol. 3, pp. 677–686.

[10] C.-M. Ong, *Dynamics Symulation of electric Machinery*. Prentice Hall Ptr, 1998, pp. 309–311.

[11] H. van Hoek; Matthias Boesing; Daniel von Treek; Timo Schoenen; Rik W. De Doncker, "Power Electronic Architectures for Electric Vehicles," *Emobility Electrical Power Train 2010*, pp. 1 –6, Nov. 2010.

[12] H. Dresig, *Schwingugen und mechanische Antriebssysteme*. Springer Berlin Heidelberg, 2006, vol. 2.

[13] M. Depenbrock, "Pulse width control of a 3-phase inverter with non-sinusoidal phase voltages." in *Conf. Rec. IEEE Industry Applications Society Int. Semiconductor Power Converter Conf, 1997*, 1997, pp. 399 –403.

[14] Alexa, D. and Lazar,A, "Optimization of pwm technique with partially constant modulating waves," *Electrical Engineering*, vol. 82, no. 5, pp. 263 –262, Oct. 2007.

[15] M. Kazmierkowski, M. Dzieniakowski, and W. Sulkowski, "Novel space vector based current controllers for pwm-inverters," *Power Electronics, IEEE Transactions on*, vol. 6, no. 1, pp. 158 –166, jan 1991.

[16] P. Clayton, *Fundamental of Electric Circuit Analysis*. John Wileyy and Sons, 2000, vol. 1.

[17] W. Latzel, *Die Methode der Betragsanpassung*. Berlin: R. Oldenbourg Verlag, 19990.

[18] R. H. Park, "Two-reaction theory of synchronous machines generalized method of analysis-part i," *American Institute of Electrical Engineers, Transactions of the*, vol. 48, no. 3, pp. 716 –727, july 1929.